



THE UNIVERSITY *of* EDINBURGH

Edinburgh Research Explorer

Conching chocolate

Citation for published version:

Blanco, E, Hodgson, DJM, Hermes, M, Besseling, R, Hunter, GL, Chaikin, PM, Cates, ME, Damme, IV & Poon, WCK 2019, 'Conching chocolate: A prototypical transition from frictionally jammed solid to flowable suspension with maximal solid content', *Proceedings of the National Academy of Sciences of the United States of America*. <https://doi.org/10.1073/pnas.1901858116>

Digital Object Identifier (DOI):

[10.1073/pnas.1901858116](https://doi.org/10.1073/pnas.1901858116)

Link:

[Link to publication record in Edinburgh Research Explorer](#)

Document Version:

Peer reviewed version

Published In:

Proceedings of the National Academy of Sciences of the United States of America

General rights

Copyright for the publications made accessible via the Edinburgh Research Explorer is retained by the author(s) and / or other copyright owners and it is a condition of accessing these publications that users recognise and abide by the legal requirements associated with these rights.

Take down policy

The University of Edinburgh has made every reasonable effort to ensure that Edinburgh Research Explorer content complies with UK legislation. If you believe that the public display of this file breaches copyright please contact openaccess@ed.ac.uk providing details, and we will remove access to the work immediately and investigate your claim.



Conching chocolate is a prototypical transition from frictionally jammed solid to flowable suspension with maximal solid content

Elena Blanco^{a,1}, Daniel J. M. Hodgson^{a,1,*}, Michiel Hermes^{a,b,1}, Rut Besseling^{a,c}, Gary L. Hunter^{d,e}, Paul M. Chaikin^d, Michael E. Cates^{a,f}, Isabella Van Damme^g, and Wilson C. K. Poon^a

^aSchool of Physics and Astronomy, The University of Edinburgh, King's Buildings, Peter Guthrie Tait Road, Edinburgh EH9 3FD, UK; ^bSoft Condensed Matter, Debye Institute for Nanomaterials Science, Utrecht University, Princetonplein 5, 3584 CC Utrecht, The Netherlands; ^cInProcess-LSP, Kloosterstraat 9, 5349 AB Oss, Netherlands; ^dCenter for Soft Matter Research (CSMR), Department of Physics, New York University; ^eExxonMobil Research and Engineering Corporate Strategic Research, 1545 Route 22 East, Annandale, New Jersey 08801; ^fDAMTP, Centre for Mathematical Sciences, Wilberforce Road, Cambridge, CB3 0WA, UK; ^gMars Chocolate UK Ltd., Dundee Road, Slough, SL1 4JX, UK

This manuscript was compiled on May 1, 2019

The mixing of a powder of 10-50 μm primary particles into a liquid to form a dispersion with the highest possible solid content is a common industrial operation. Building on recent advances in the rheology of such 'granular dispersions', we study a paradigmatic example of such powder incorporation: the conching of chocolate, in which a homogeneous, flowing suspension is prepared from an inhomogeneous mixture of particulates, triglyceride oil and dispersants. Studying the rheology of a simplified formulation, we find that the input of mechanical energy and staged addition of surfactants combine to effect a considerable shift in the jamming volume fraction of the system, thus increasing the maximum flowable solid content. We discuss the possible microscopic origins of this shift, and suggest that chocolate conching exemplifies a ubiquitous class of powder-liquid mixing.

Chocolate | Rheology | Jamming | Incorporation

The incorporation of liquid into dry powder with primary particle size in the granular range ($\sim 10\text{-}50\ \mu\text{m}$) to form a flowing suspension with solid volume fraction $\phi \gtrsim 50\%$ is important in many industries [1]. Often, maximising solid content is a key goal. Cements for building or bone replacement and ceramic 'green bodies' are important examples, where higher ϕ improves material strength [2]. Another example is chocolate manufacturing, where high solid content (= lower fat [3]) is achieved by 'conching'.

Conching [4], invented by Rodolphe Lindt in 1879, is important for flavor development, but its major physical function is to turn an inhomogeneous mixture of particulates (including sugar, milk solids and cocoa solids) and cocoa butter (a triglyceride mixture) into a homogeneous, flowing suspension (liquid chocolate) by prolonged mechanical action and the staged addition of dispersants. In this paper, we focus on this effect, and seek to understand how mechanical action and dispersants together transform a non-flowing, inhomogeneous mixture into a flowing suspension, a process that has analogs in, e.g., the ceramics and pharmaceuticals sectors [1].

We find that the key physical processes are friction-dominated flow and jamming. Specifically, two of the key rheological parameters in chocolate manufacturing, the yield stress, σ_y , and the high-shear viscosity, η_2 , are controlled by how far the volume fraction of solids, ϕ , of the chocolate formulation is situated from the jamming volume fraction, ϕ_J . We demonstrate that the first part of the conche breaks apart particulate aggregates, thus increasing ϕ_J relative to the fixed mass fraction. In the second part of the conche, the addition of a small amount of dispersant reduces the inter-particle friction and further raises ϕ_J , in turn reducing σ_y and η_2 , resulting in

fluidization of the suspension, i.e. a solid to liquid transition. Such ' ϕ_J engineering' is common to diverse industries that rely on the production of high-solid-content dispersions.

Shear thickening suspensions

We first review briefly recent advances in granular suspension rheology [5–14]. The viscosity of a high- ϕ granular suspension increases from a low-stress Newtonian value when the applied stress, σ , exceeds some onset stress, σ^* , reaching a higher Newtonian plateau at $\sigma \gg \sigma^*$: the suspension shear thickens. The low- and high-stress viscosities, η_1 and η_2 , diverge as

$$\eta_r = A \left(1 - \frac{\phi}{\phi_J^\mu(\sigma)} \right)^{-\lambda}, \quad [1]$$

where $\eta_r = \eta_{1,2}/\eta_0$ with η_0 the solvent viscosity, $A \simeq 1$, and $\lambda \simeq 2$ for spheres [15, 16]. The jamming point, ϕ_J , is a function of both the inter-particle friction coefficient, μ , and the applied stress, σ . The latter begins to press particles into contact when it exceeds σ^* . With $\mu \rightarrow 0$, no shear thickening is observed, and η_r diverges at random close packing, $\phi_J = \phi_{\text{rcp}}$. At finite μ , the low-stress viscosity $\eta_1(\phi)$ still diverges at ϕ_{rcp} , but $\eta_2(\phi)$, the high-stress viscosity, now diverges at some $\phi_J = \phi_m^\mu < \phi_{\text{rcp}}$. For monodisperse hard spheres, Figure 1(a), $\phi_{\text{rcp}} \approx 0.64$ and $\phi_m^{\mu \rightarrow \infty} \approx 0.54$ (where ' ∞ ' in practice means $\mu \gtrsim 1$) [8, 17]. (Below we drop the ' μ ' in ϕ_m^μ unless it is needed.) A granular suspension at $\phi > \phi_m$ cannot flow at high stress either steadily

Significance Statement

Chocolate conching is the process in which an inhomogeneous mixture of fat, sugar and cocoa solids is transformed into a homogeneous flowing liquid. Despite the popularity of chocolate and the antiquity of the process, until now there has been poor understanding of the physical mechanisms involved. Here, for the first time, we show that two of the main roles of conching are the mechanical breakdown of aggregates and the reduction of inter-particle friction through the addition of a dispersant. Intriguingly, the underlying physics we describe is related to the popular stunt of 'running on cornstarch'.

Author contributions: WP, PC, MH, MC and IVD conceptualised the work. EB, DH, GH and RB performed experiments. EB, DH, MH, RB and GH analysed and interpreted data. DH and WP prepared the manuscript.

Conflict of interest statement: This work was funded by Mars Chocolate UK Ltd..

¹EB, DH and MH contributed equally to this work.

*To whom correspondence should be addressed. E-mail: danieljmhodgson@gmail.com

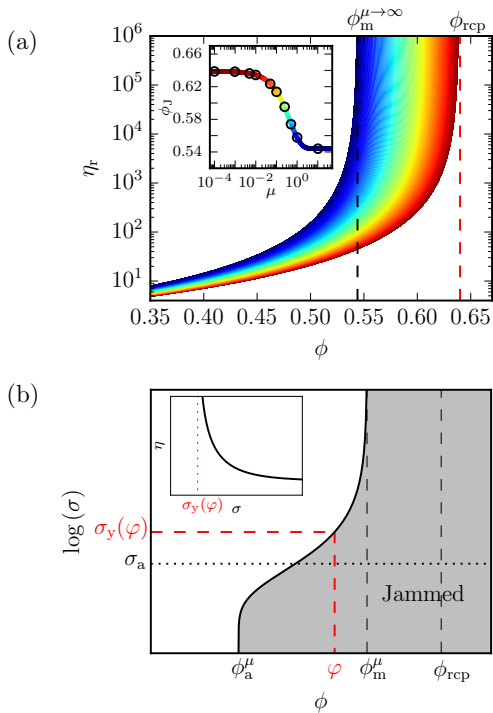


Fig. 1. (a) The high-shear viscosity of suspensions of granular hard spheres normalised by the solvent viscosity, η_r , plotted against the volume fraction ϕ , with friction coefficient increasing from $\mu = 0$ (red), diverging at ϕ_{rcp} , to $\mu \rightarrow \infty$ (blue), diverging at $\phi_m^{\mu \rightarrow \infty}$. Inset: The jamming volume fraction, ϕ_J , where η_r diverges, as a function of the coefficient of static friction μ (replotted from [17]). (b) The jamming state diagram of a frictional granular suspension with inter-particle adhesion. The adhesive strength is set by $\sigma_a \gg \sigma^*$. Shaded region = jammed. The flow curve of a suspension with volume fraction φ is shown in the inset: it has a yield stress $\sigma_y(\varphi)$.

or homogeneously [12]: it shear-jams [7]. Instead, theory [7] and experiments [18] suggest that it granulates.

The onset stress, σ^* , correlates with the force to overcome an inter-particle repulsive barrier; typically $\sigma^* \sim d^{-\nu}$ with $\nu \lesssim 2$, where d is the particle diameter [9]. For granular suspensions, σ^* is far below stresses encountered in liquid-powder mixing processes, so that they always flow with viscosity $\eta_2(\phi, \mu)$, which diverges at $\phi_m < \phi_{rcp}$. To formulate a flowable granular suspension with maximum solid content is therefore a matter of maximising ϕ_m , e.g., by lowering μ , Figure 1(a) (inset).

Inter-particle adhesion introduces another stress scale, σ_a , characterising the strength of adhesive interactions [19]. A yield stress, σ_y , emerges above some $\phi_a^\mu < \phi_m^\mu$ that is dependent on both adhesion and friction [19, 20] (hence the μ superscript, which, again, we will drop unless needed), and diverges at ϕ_m^μ .

Competition between friction and adhesion gives rise to a range of rheologies [19]. If $\sigma^*/\sigma_a \ll 1$, the suspension shear thins at $\sigma > \sigma_y$ to the frictional viscosity, η_2 . The state diagram such a system is shown schematically in Figure 1(b); the inset shows a typical flow curve. However, a suspension with $\sigma^*/\sigma_a \gg 1$ first shear thins at $\sigma > \sigma_y$, and then shear thickens as σ exceeds σ^* . Modifying system additives (e.g. removing polymeric depletants or adding surfactants) can increase σ^*/σ_a and change the first type of behavior to the second type [21, 22].

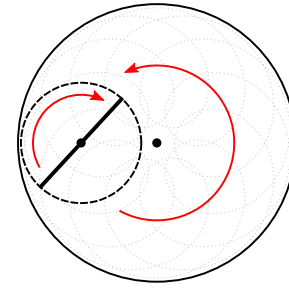


Fig. 2. Schematic of a planetary mixer. A blade (bold) rotates inside a bowl, full circle, which counter rotates. Shearing occurs in the gap between the blade and the bowl.

Conching phenomenology

We worked with a simplified chocolate formulation of ‘crumb powder’ dispersed in sunflower oil with lecithin [23]. For one experiment, we also added a second surfactant, polyglycerol polyricinoleate (PGPR). Crumb is manufactured by drying a water-based mixture of sucrose crystals, milk and cocoa mass followed by milling [24]. To perform a laboratory-scale conche, we used a planetary mixer, Figure 2, to prepare 500 g batches. The total lecithin added was 0.83 wt%. In the first step, the ‘dry conche’, we mixed the solids with the oil and 0.166 wt% of lecithin (20% of the total) in the planetary mixer at ≈ 100 rpm until the material smears around the bowl right after it has cohered into a single lump around the blade. At $\phi = 0.55$, this took ≈ 40 min. Then, for the ‘wet conche’, the remaining lecithin was added and mixed for a further 20 min.

Conched samples were prepared with solid concentrations in the range $0.4 \lesssim \phi \lesssim 0.6$, with ϕ calculated using measured densities (see Materials and Methods), so that a weight fraction of 74% converts to $\phi = 0.55$ (assuming all the fat contained in the crumb melts during conching). In each case, the flow curves of the as-conched sample as well as that of samples successively diluted with pure oil were measured using parallel-plate rheometry (see Materials and Methods).

Figure 3 (A-H) show the phenomenology of conching a mixture with solid volume fraction¹ $\phi_0 = 0.55$ (or 74 wt.%) to which initially 20% of the final total of 0.83 wt.% of lecithin has been added; the accompanying plots show the power consumption of the planetary mixer as well as measured densities of the sample as conching proceeds. Almost immediately after addition of the sunflower oil to the crumb powder ($t = 0$ min), all the liquid appeared to have been absorbed. The sample then proceeded to granulate, with the granule size increasing with time. The first granules were visually matt and dry, Figure 3, A-C, and do not stick to each other during mixing.

The skeletal density of a material, Figure 3 (red-box inset in plot and Materials and Methods), is the mass of mesoscopic condensed phases (solids and liquids) it contains divided by the volume occupied by these phases, and therefore excludes externally connected air pores. The skeletal density sharply decreased during the first few minutes, converging rapidly to the system average bulk density of the solid and liquid components. The envelope density, Figure 3 (blue-box inset in plot and Materials and Methods), defined as the mass of a sample divided by its macroscopic volume, including air- and liquid-filled pores, increased over the first 15 min as the

¹That is, the ratio of solid volume to total solid plus liquid volume, discounting any air that may be present; this differs from the granulation literature, where the air is typically taken into account.

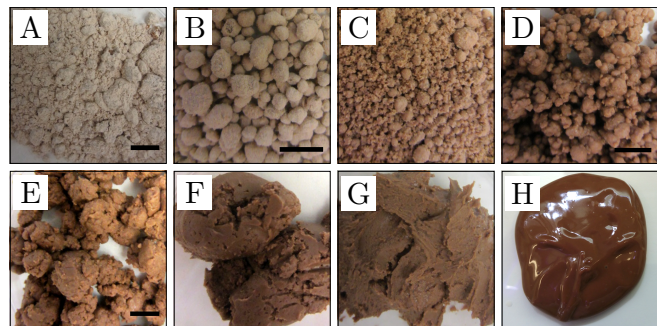
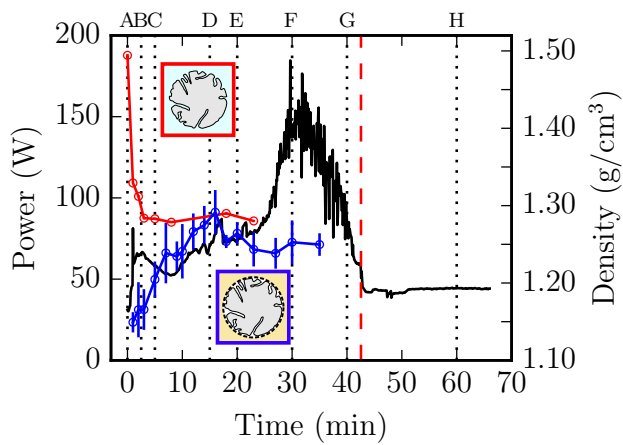


Fig. 3. *Top* Power consumption (—), skeletal density (—) and envelope density (—) as a function of mixing time for a typical model chocolate formulation with $\phi_0 = 0.55$ ($\equiv 74$ wt.%). Red box: the density of the grey shaded cluster is the skeletal density. Blue box: the average density inside the black dashed circle is the envelope density. Red dash line denotes time at which second shot of lecithin is added and the transition from dry to wet conche. *Bottom* Visual appearance of samples taken out of the planetary mixer at various stages of the conche. Letter labels correspond in the upper and lower panels. Scale bars are 10 mm. Granule size increases A–E; by F, the granule size has diverged to the size of the system.

granules compacted, and converged to the skeletal density. The power consumption increased slowly.

After ≈ 15 min the granules became visibly moist and coalesced into larger ‘raspberry-like’ structures, Figure 3(D), that somewhat resemble washing powder manufactured by granulation [25]. The envelope density decreased slightly, presumably due to air incorporation as granules coalesced, and then remained constant: compactification had finished by stages E and F. The power consumption sharply peaked at ≈ 30 min, when all of the material had formed into a ball adhering to the blade. Thereafter, the power consumption rapidly decreased, and the material became a paste that did not flow easily, Figure 3(G). Soon after this (red dashed line in the plot) the remaining 80% of lecithin is added, and the ‘dry conche’ transitions to the ‘wet conche’. The sample rapidly fluidised into a glossy, pourable suspension, Figure 3(H). A sharp decrease in power consumption accompanied this fluidisation. Note that the consumed power as a function of time is highly reproducible, in both the total power consumed and the time required to reach the peak, provided the same batch of powder is used.

Similar phenomenology is widely reported in wet granulation [25], where liquid is gradually added to a dry powder

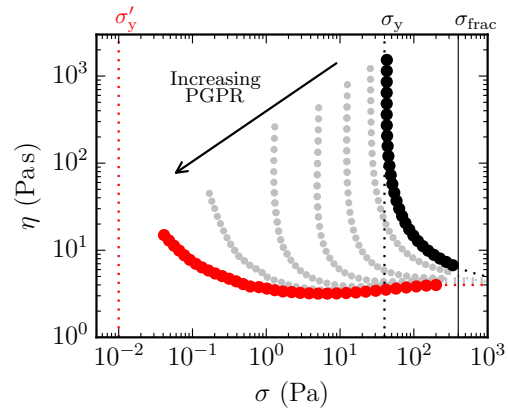


Fig. 4. Model chocolate flow curves. (●): $\sigma^*/\sigma_a \ll 1$, crumb conched with 0.83% lecithin ($\phi_0 = 0.55$). (●): $\sigma^*/\sigma_a \gg 1$; as before, but with 1.2% PGPR. Intermediate curves for intermediate PGPR contents. Dashed lines guide the eye to high-shear viscosity at $\sigma > \sigma_{\text{frac}}$.

to manufacture granules for applications ranging from agrochemicals to pharmaceuticals. A similar sequence of events to that in Figure 3 A–H is seen as the amount of added liquid increases. However, the system would typically become ‘over-wet’, i.e. turn into a flowing suspension, at the peak of the power curve (equivalent to our stage F) [26], rather than later (as in our case, at stage H). We note especially that there is a striking visual similarity in the time-lapsed images and power curves for concrete mixing at fixed liquid content [27]. Such similarities across diverse sectors suggest that the incorporation of liquid into powder to form a flowing suspension via various stages of granulation may be underpinned by generic physics, which we seek to uncover through rheology.

Effect of conching on chocolate rheology

Figure 4 (●) shows the flow curve, $\eta(\sigma)$, of a fully-conched crumb mixture with $\phi_0 = 0.54$ (73 wt.%). Below a yield stress, $\sigma_y \approx 40$ Pa, $\eta \rightarrow \infty$. Above σ_y the sample shear thins towards a Newtonian plateau at $\lesssim 5$ Pa s. However, just before reaching this value, the surface of the sample breaks up and it is no longer contained between the rheometer tools. This occurs at an approximately ϕ_0 -independent $\sigma_{\text{frac}} \approx 400$ Pa, close to the stress, $\sim 0.1\Sigma/a$ (≈ 300 Pa for our system with $a \approx 10$ μm and surface tension $\Sigma \approx 30$ mN m $^{-1}$), where particles may be expected to poke out of the free suspension-air interface [28].

Interestingly, if PGPR is added together with the ‘second shot’ of lecithin at the beginning of the wet conche, a different rheology is obtained, Figure 4 (●): σ_y is dramatically lowered (here, to $\sigma'_y \sim 10^{-2}$ Pa), revealing shear thickening with an onset stress of $\sigma^* \gtrsim 2$ Pa. This suggests that in the sample conched with lecithin only, shear thickening is masked [19, 21, 22] by $\sigma_y > \sigma^*$, but the high-shear viscosity is nevertheless the shear-thickened, frictional-contacts dominated η_2 .

This high-shear viscosity, $\eta_{\text{fc}}^{[\phi_0]}$, of model chocolates fully-conched (fc) with lecithin at nine different solid fractions, ϕ_0 , is plotted in Figure 5(a) (○). In four cases, we successively diluted the conched samples with sunflower oil and measured the high-shear viscosity along each dilution series, $\eta_{\text{fc}}^{[\phi_0]}(\phi)$. Each data set can be fitted to Equation 1 with $A = 1$, Figure 5(a) (solid lines), confirming what is already obvious from inspection, viz.,

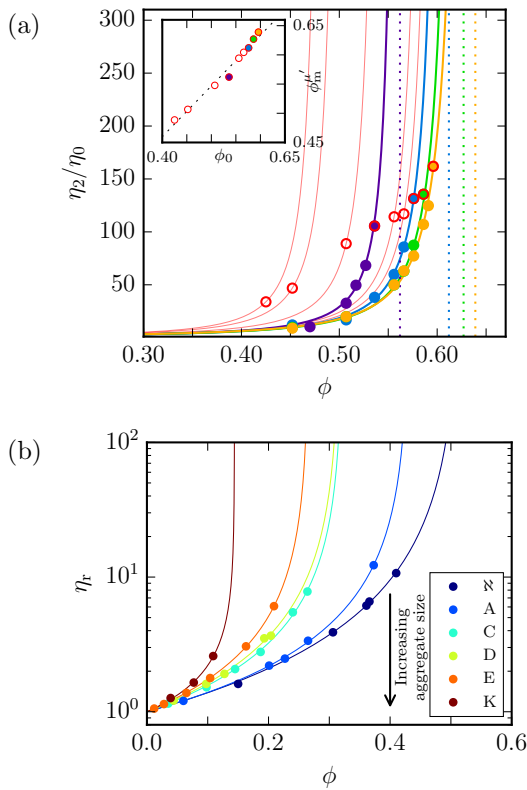


Fig. 5. (a) Relative high shear viscosity of chocolate suspensions *vs* solid volume fraction. (○): $\eta_{fc}^{[\phi_0]}$, suspensions fully conched in the planetary mixer. Filled circles: Diluted fully-conched suspensions: (●): diluted from $\phi_0 = 0.596$. (●): diluted from $\phi_0 = 0.586$. (●): diluted from $\phi_0 = 0.576$. (●): diluted from $\phi_0 = 0.536$. Matching-color vertical dotted lines: ϕ_m from fitting Equation 1 to these four data sets. Thin red curves: Equation 1 with $\lambda = 1, 73$ consistent with single open red circle data points. Inset Frictional jamming ϕ_m of chocolate suspensions as a function of the conched volume fraction ϕ_0 . Symbols as in main figure. (b) Replotted data of Lewis and Nielson [29] for 30-40 μm glass spheres suspended in Aroclor, with each data set fitted to Equation 1; aggregate size increases from N and then A to K.

that these data sets diverge at different points: ● $\phi_m = 0.639$ ($\lambda = 1.88$) for $\phi_0 = 0.596$, ● $\phi_m = 0.627$ ($\lambda = 1.78$) for $\phi_0 = 0.586$, ● $\phi_m = 0.612$ ($\lambda = 1.72$) for $\phi_0 = 0.576$, ● $\phi_m = 0.562$ ($\lambda = 1.53$) for $\phi_0 = 0.536$. In each remaining case, we estimate ϕ_m without generating a full dilution series at each ϕ_0 by fitting Equation 1 through each of the five $\eta_{fc}^{[\phi_0]}$ data points using the averaged exponent from the four full dilution series $\lambda = \bar{\lambda} = 1.73$, Figure 5(a) (thin red curves).

Plotting all available pairs of (ϕ_0, ϕ_m) , Figure 5(a) (inset), confirms that ϕ_m increases as we conche the mixtures at higher solid fraction ϕ_0 . That is to say, conching at a higher solid fraction gives rise to a higher jamming volume fraction. There is, however, an upper bound to such ϕ_m optimisation, which we can estimate by noting that, empirically, $\phi_m(\phi_0)$ is approximately linear in our range of ϕ_0 . A linear extrapolation shows that $\phi_m = \phi_0$ at $\phi_0^{\text{max}} \approx 0.8$. This is likely an overestimate: the approximately linear relation shown in the inset of Figure 5(a) probably becomes sub-linear and perhaps saturates at higher ϕ_0 . Nevertheless, the existence of some $\phi_0^{\text{max}} < 0.8$ beyond which conching will not increase ϕ_m seems to be a reasonable inference from our data.

Conching as jamming engineering

Conching reduces aggregate size and increases ϕ_m . Interestingly, our observations may be interpreted in terms of an ‘inverse conching’ experiment performed some 50 years ago. Lewis and Nielsen [29] measured the viscosity of 30-40 μm glass spheres suspended in Aroclor (a viscous Newtonian organic liquid) as a function of volume fraction, Figure 5(b) (data set N), and repeated the measurements with glass beads that have been increasingly aggregated by sintering before dispersal in Aroclor, Figure 5(b), giving average number of primary particles in an aggregate N of 1.8 (A), 5 (C), 8 (D), 12 (E) and 200-300 (K). Neutral silica in an apolar solvent likely has a vanishingly small σ^* , so that Lewis and Nielsen were measuring $\eta_2(\phi)$, the shear-thickened viscosity, which diverges at ϕ_m . Thus, ϕ_m is clearly lowered by aggregation.

We interpret our data, Figure 5(a), as ‘Lewis and Nielsen in reverse’. The primary particles in raw crumb are aggregated in storage due to moisture, etc. [30]. Conching reduces aggregation and therefore increases ϕ_m , with the effect being progressively more marked as the material is being conched at higher ϕ_0 . The latter effect is probably because the same external stress generates higher particle pressure at higher ϕ [12, 31], which breaks up aggregates more effectively.

The linear relation in the inset of Figure 5(a) extrapolates to a finite intercept at $(0, 0.11 \pm 0.02)$, suggesting that the viscosity of unconched crumb powder would diverge at $\phi_m = 0.11$. This value is perhaps unrealistically low: the real $\phi_m(\phi_0)$ dependence probably becomes sub-linear at low ϕ_0 and saturates at some value > 0.11 . Nevertheless, there seems little doubt that unconched, aggregated crumb suspensions jam at volume fractions considerably below those used for real chocolate formulations ($\phi_0 \gtrsim 0.55$).

The change in aggregation during the liquid-powder mixing process is often monitored by laser light scattering. This method would not have separated Lewis and Nielsen’s samples N, A, C, D and E. Highly accurate data at very low scattering angles are needed to distinguish N -mers with small N even when the primary particles are quasi-monodisperse. (See the instructive study of monomers and dimers by Johnson *et al.* [32].) Similarly, light scattering will be at best a crude tool for studying conching. In fact, measuring changes in ϕ_m by rheology is likely a good, albeit indirect, method to detect changes in low N -mer aggregation.

From granules to flowing suspension. We can now describe the whole conching process in terms of suspension rheology. Consider a crumb-oil-lecithin mixture at $\phi_0 = 0.576$, somewhat higher than in Figure 3. The jamming point of the initial mixture at time $t = 0$, ϕ_m^{init} , is substantially lower (our lower-bound estimate, the y -intercept of Figure 5(a) (inset), being 0.11). This initial mixture therefore cannot flow homogeneously. In state-diagram terms, the starting system is deep inside the jammed region, Figure 6(a), where, under mechanical agitation, it granulates [7], Figure 3 (B-D). These granules form as a result of there being insufficient liquid to saturate the entire system, and are held together by a combination of surface tension maintaining a jammed particle packing and inter-particle adhesion. The granulation process is controlled by the kinetics of cluster-cluster collisions and the mechanical properties of the clusters [25, 33, 34]. In parallel, aggregates are being broken up, increasing the free volume in the system,

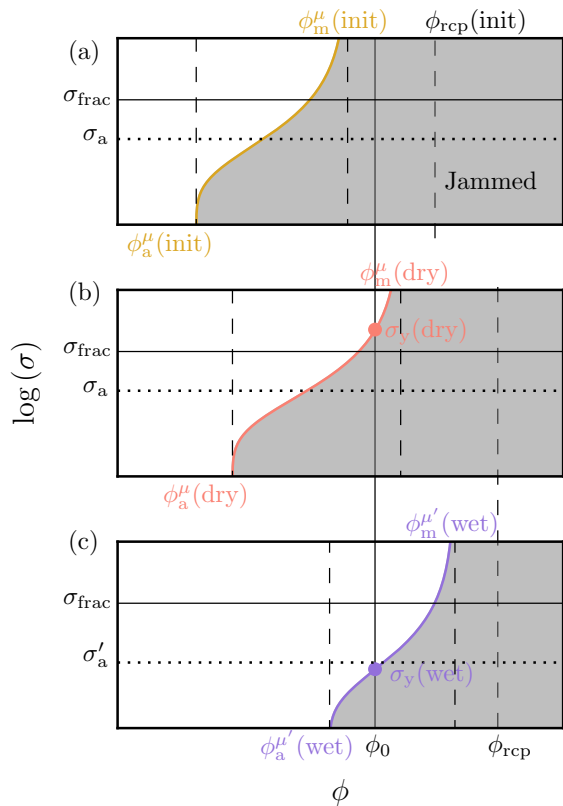


Fig. 6. The conching process represented as shifts in the jamming state diagram (cf. Figure 1(b)). (a) The formulation at ϕ_0 is considerably more concentrated than the jamming point of the unconched suspension, $\phi_m^{\mu}(\text{init})$. (b) It granulates under mechanical agitation, simultaneously breaking up aggregates and increasing both ϕ_m^{μ} and ϕ_a^{μ} , thus shifting the jamming boundary to the right. At the end of the dry conche, the suspension could in principle flow, $\phi_0 < \phi_m^{\mu}(\text{dry})$, but in fact cannot do so, because $\sigma_{\text{frac}} < \sigma_y(\text{dry})$. (c) Addition of the ‘second shot’ of lecithin reduces the inter-particle friction coefficient to $\mu' < \mu$ and the adhesive interaction to $\sigma'_a < \sigma_a$, thereby shifting the jamming boundary further to the right and down, dropping $\sigma_y(\text{wet})$ below σ_{frac} . Since ϕ_0 is now considerably below $\phi_m^{\mu}(\text{wet})$, the system is now a flowing suspension.

so that both ϕ_m^{μ} and ϕ_a^{μ} steadily increase, until ϕ_m^{μ} just exceeds ϕ_0 .

At this point, the system becomes fully saturated and we may expect the system to turn into a flowable suspension, albeit with a very high viscosity, since there is no longer a shear jammed state for surface tension to maintain. This is indeed what happens in many systems: the power is observed to peak just as the material becomes (in granulation jargon) ‘overwet’ [26], i.e. a flowing suspension with a shiny surface. In our case, at the power peak (stage F in Figure 3), the suspension still does not flow easily and appears visually matt. This is probably because the sample fractures before it can yield to flow homogeneously, i.e., $\sigma_y > \sigma_{\text{frac}}$ (cf. the earlier discussion of σ_{frac} associated with Figure 4).

Further conching continues to increase ϕ_m until at the end of the dry conche, the yield stress, $\sigma_y(\text{dry})$, only just exceeds the fracture stress, σ_{frac} , Figure 6(b). Here, the addition of the ‘second shot’ of lecithin has a dramatic effect. We suggest that this is because the additional lecithin lowers μ and σ_a to μ' and σ'_a . The jamming boundary abruptly shifts to the right and drops down, Figure 6(c). The resulting dramatic lowering

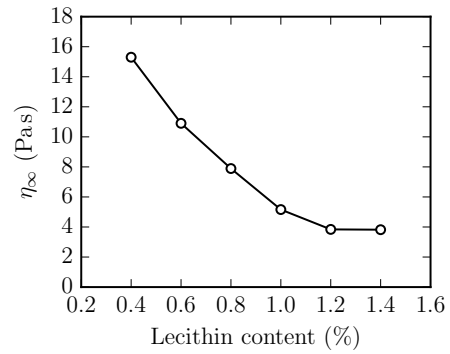


Fig. 7. High-shear viscosity of model chocolate at $\phi_0 = 0.557$ dry-conched without lecithin as a function of subsequently-added lecithin.

of the yield stress to $\sigma_y(\text{wet}) < \sigma_{\text{frac}}$ in a system where, now, ϕ_0 is considerably below $\phi_m(\text{wet})$, immediately produces a flowing suspension, liquid chocolate.

Lecithin as a lubricant. We have suggested that the lecithin added in the ‘second shot’ lowers μ and therefore increases both ϕ_m^{μ} and ϕ_a^{μ} by releasing constraints on the system [19]. To provide direct experimental evidence for this role, we prepared a dry conche with the first shot of lecithin omitted, which again produced a non-flowing paste. Various amounts of lecithin was mixed into aliquots of this paste, which liquified. The high-shear viscosity, η_2 , of the resulting suspensions decreases with lecithin concentration, Figure 7. To check that this was not due to the oils in lecithin lowering the sample volume fraction, we repeated the experiment added an equivalent volume of oil corresponding to the maximum lecithin concentration (1.4%). This failed to liquify the paste. We may therefore conclude that lecithin causes this effect by lowering μ and so increasing the jamming point, $\phi_J = \phi_m^{\mu}$, Figure 1 (inset).

Summary and conclusions

Creating flowable solid-in-liquid dispersions of maximal solid content is a generic goal across many industrial sectors. We have studied one such process in detail, the conching of crumb powder and sunflower oil into a flowing model chocolate. We interpreted our observations and measurements using existing knowledge from the granulation literature as well as an emerging new understanding of shear thickening and jamming in granular dispersions. The resulting picture is summarised in Figure 6. The essential idea is that conching, and more generally wet milling, is about ‘jamming engineering’ – manipulating ϕ_m^{μ} and ϕ_a^{μ} by changing the state of aggregation, and ‘tuning’ the inter-particle friction coefficient μ and the strength of inter-particle adhesion, σ_a . Importantly, many additives ostensibly acting as dispersants to reduce inter-particle attraction and so lower σ_a may, in fact, function primarily as lubrications to lower μ and so increase ϕ_m . Our scheme, Figure 6, with appropriate shifts in σ_{frac} , can be used to understand liquid incorporation into powders in many different specific applications.

Our proposed picture for conching/wet milling poses many questions. For example, the rheology of a suspension at the end of dry conche, in which flow is in principle possible ($\phi_0 < \phi_m$) but in practice ruled out by surface fracture occurring

before bulk yielding, has not yet been studied in any detail. Neither is the role of changing ϕ_m during the granulation process understood. Our results therefore constitute only a first step towards a unified description of liquid incorporation, wet milling and granulation.

Materials and Methods

Our crumb powder (supplied by Mars Chocolate UK) consists mostly of faceted particles with mean radius $a \approx 10 \mu\text{m}$ (polydispersity $\gtrsim 150\%$) according to laser diffraction (Beckman-Coulter LS-13 320). It has a density 1.453 g cm^{-3} and a specific (BET) surface area $2.02 \text{ m}^2 \text{ g}^{-1}$ (data provided by Mars Chocolate UK). We used sunflower as purchased (Flora) and soy lecithin as supplied (by Mars Chocolate UK). The latter consists of a mixture of phospholipids ($\approx 60\%$) with some residual soya oil. Our sunflower oil was Newtonian at 20°C , with viscosity $\eta_0 = 54 \text{ mPa}\cdot\text{s}$. Its density was measured by an Anton Paar DMA density meter to be 0.917 g cm^{-3} . Using sunflower oil rather than cocoa butter obviates the need for heating during rheological measurements. The rheology of the chocolate suspension obtained from conching our mixture resembles that of fresh liquid chocolate made using cocoa

butter [23]. Our PGPR was also supplied by Mars Chocolate UK.

Conching was performed using a Kenwood kMix planetary mixer with a K-blade attachment, adding the lecithin in two successive batches as described in the main text. We measured the skeletal density at various stages of conching by performing helium pycnometry (Quantachrome Ultrapyc). The envelope density was measured using a $2.00 \pm 0.02 \text{ ml}$ Pyrex micro-volumetric flask with sunflower oil as the liquid phase.

Rheometric measurements were performed using a stress-controlled rheometer (TA Instruments, DHR-2) in a cross-hatched plate-plate geometry (diameter 40 mm , $1 \times 1 \times 0.5 \text{ mm}$ serrated grid of truncated pyramids) to minimise wall slip, at a gap height of 1 mm and a temperature of 20°C .

All data plotted in this work can be downloaded from <https://doi.org/10.7488/ds/2515>.

ACKNOWLEDGMENTS. We thank Mars Chocolate UK Ltd. for initiating and funding part of this work. Other funding came from the EPSRC (EP/J007404/1 and EP/N025318/1). Research at NYU was supported partially by the MRSEC Program of the National Science Foundation under Award Number DMR-1420073. We thank Ben Guy, John Royer and Jin Sun (Edinburgh) and Will Taylor (Mars Chocolate) for illuminating discussions.

- Kaye B (1997) *Powder Mixing*. (Springer Netherlands).
- Carneim TJ, Green DJ (2004) Mechanical properties of dry-pressed alumina green bodies. *J. Am. Ceramic Soc.* 84:1405–1410.
- Tao R, Tang H, Tawhid-Al-Islam K, Du E, Kim J (2016) Electrorheology leads to healthier and tastier chocolate. *Proc. Natl. Acad. Sci. (USA)* 113:7399–7402.
- Gutiérrez TJ (2017) State-of-the-art chocolate manufacture: A review. *Comp. Rev. Food Safety* 16:1313–1344.
- Seto R, Mari R, Morris JF, Denn MM (2013) Discontinuous shear thickening of frictional hard-sphere suspensions. *Phys. Rev. Lett.* 111:218301.
- Wyart M, Cates ME (2014) Discontinuous shear thickening without inertia in dense non-Brownian suspensions. *Phys. Rev. Lett.* 112:098302.
- Cates ME, Wyart M (2014) Granulation and bistability in non-Brownian suspensions. *Rheol. Acta* 53:755–764.
- Mari R, Seto R, Morris JF, Denn MM (2014) Shear thickening, frictionless and frictional rheologies in non-Brownian suspensions. *J. Rheol.* 58(6):1693–1724.
- Guy BM, Hermes M, Poon WCK (2015) Towards a unified description of the rheology of hard-particle suspensions. *Phys. Rev. Lett.* 115:088304.
- Lin NY et al. (2015) Hydrodynamic and contact contributions to continuous shear thickening in colloidal suspensions. *Phys. Rev. Lett.* 115:228304.
- Royer JR, Blair DL, Hudson SD (2016) Rheological signature of frictional interactions in shear thickening suspensions. *Phys. Rev. Lett.* 116:188301.
- Hermes M et al. (2016) Unsteady flow and particle migration in dense, non-Brownian suspensions. *J. Rheol.* 60:905–916.
- Comtet J et al. (2017) Pairwise frictional profile between particles determines discontinuous shear thickening transition in non-colloidal suspensions. *Nat. Commun.* 8:15633.
- Clavaut C, Béruit A, Metzger B, Forterre Y (2017) Revealing the frictional transition in shear thickening suspensions. *Proceedings of the National Academy of Sciences* p. 201703926.
- Maron SH, Pierce PE (1956) Application of ree-eyring generalized flow theory to suspensions of spherical particles. *J. Colloid Sci.* 11:80–95.
- Krieger IM, Dougherty TJ (1959) A mechanism for non-newtonian flow in suspensions of rigid spheres. *Trans. Soc. Rheol.* 3:137–152.
- Silbert LE (2010) Jamming of frictional spheres and random loose packing. *Soft Matter* 6(13):2918–2924.
- Hodgson DJM, Hermes M, Poon WCK (2015) Jamming and the onset of granulation in a model particle system. *arXiv:1507.08098*.
- Guy BM, Richards JA, Hodgson DJM, Blanco E, Poon WCK (2018) Constraint-based approach to granular dispersion rheology. *Phys. Rev. Lett.* 121(12):128001.
- Liu W, Jin Y, Chen S, Makse HA, Li S (2017) Equation of state for random sphere packings with arbitrary adhesion and friction. *Soft Matter* 13(2):421–427.
- Gopalakrishnan V, Zukoski C (2004) Effect of attractions on shear thickening in dense suspensions. *Journal of Rheology* 48(6):1321–1344.
- Brown E et al. (2010) Generality of shear thickening in dense suspensions. *Nature Mater.* 9(3):220.
- Taylor JE, Van Damme I, Johns ML, Routh AF, Wilson DI (2009) Shear rheology of molten crumb chocolate. *J. Food Sci.* 74:55–61.
- Beckett ST (2003) Is the taste of british milk chocolate different. *Int. J. Dairy Tech.* 56:139–142.
- Salman AD, Hounslow M, Seville JP, eds. (2006) *Granulation*, Handbook of Powder Technology. (Elsevier) Vol. 11.
- Betz G, Bürgin PJ, Leuenberger H (2003) Power consumption profile analysis and tensile strength measurements during moist agglomeration. *Int. J. Pharm.* 252(1):11–25.
- Cazacliu B, Roquet N (2009) Concrete mixing kinetics by means of power measurement. *Cement Concrete Res.* 39:182–194.
- Brown E, Jaeger HM (2014) Shear thickening in concentrated suspensions: phenomenology, mechanisms and relations to jamming. *Rep. Prog. Phys.* 77(4):046602.
- Lewis TB, Nielsen LE (1968) Viscosity of dispersed and aggregated suspensions of spheres. *Trans. Soc. Rheol.* 12:421–443.
- Pietsch W (2004) *Agglomeration in Industry, 2 Volume Set: Occurrence and Applications*. (John Wiley & Sons).
- Boyer F, Guazzelli É, Pouliquen O (2011) Unifying suspension and granular rheology. *Phys. Rev. Lett.* 107:188301.
- Johnson PM, van Kats CM, van Blaaderen A (2005) Synthesis of colloidal silica dumbbells. *Langmuir* 21(24):11510–11517.
- Iverson SM, Litster JD (1998) Growth regime map for liquid-bound granules. *AIChE J.* 44:1510–1518.
- Iverson S et al. (2001) Growth regime map for liquid-bound granules: Further development and experimental validation. *Powder Technol.* 117:83–97.